



Observed soil temperature trends associated with climate change in the Tibetan Plateau, 1960–2014

Xuewei Fang^{1,2} · Siqiong Luo² · Shihua Lyu^{1,3}

Received: 7 November 2016 / Accepted: 23 November 2017 / Published online: 12 January 2018
© The Author(s) 2018. This article is an open access publication

Abstract

Soil temperature, an important indicator of climate change, has rarely explored due to scarce observations, especially in the Tibetan Plateau (TP) area. In this study, changes observed in five meteorological variables obtained from the TP between 1960 and 2014 were investigated using two non-parametric methods, the modified Mann–Kendall test and Sen’s slope estimator method. Analysis of annual series from 1960 to 2014 has shown that surface (0 cm), shallow (5–20 cm), deep (40–320 cm) soil temperatures (ST), mean air temperature (AT), and precipitation (P) increased with rates of 0.47 °C/decade, 0.36 °C/decade, 0.36 °C/decade, 0.35 °C/decade, and 7.36 mm/decade, respectively, while maximum frozen soil depth (MFD) as well as snow cover depth (MSD) decreased with rates of 5.58 and 0.07 cm/decade. Trends were significant at 99 or 95% confidence level for the variables, with the exception of P and MSD. More impressive rate of the ST at each level than the AT indicates the clear response of soil to climate warming on a regional scale. Monthly changes observed in surface ST in the past decades were consistent with those of AT, indicating a central place of AT in the soil warming. In addition, with the exception of MFD, regional scale increasing trend of P as well as the decreasing MSD also shed light on the mechanisms driving soil trends. Significant negative-dominated correlation coefficients ($\alpha = 0.05$) between ST and MSD indicate the decreasing MSD trends in TP were attributable to increasing ST, especially in surface layer. Owing to the frozen ground, the relationship between ST and P is complicated in the area. Higher P also induced higher ST, while the inhibition of freeze and thaw process on the ST in summer. With the increasing AT, P accompanied with the decreasing MFD, MSD should be the major factors induced the conspicuous soil warming of the TP in the past decades.

1 Introduction

It is widely accepted that the Earth has warmed (IPCC 2007). Climate warming is widespread over the world and is greater at higher latitudes. Furthermore, land regions have warmed faster than the oceans (Qian et al. 2011). Observations have unearthed

the impacts of climate warming on ecosystem and natural resources. Some examples are the degradation of frozen grounds, glacial recession, a trend in decreasing snow coverage, and the expansionist number of glacial lakes. With rapid retreat and thinning of permafrost, large carbon pools sequestered in permafrost could be released to increase net sources of atmospheric carbon, creating a positive feedback and accelerated warming (Yang et al. 2010a). Snow cover strongly interacts with climate through snow albedo feedbacks (Niu and Yang 2007). Changes in snow coverage on the earth are bound to create a new energy equilibrium in the earth atmosphere system. In addition, the glacial retreat also has an important impact on the water resource of the arid regions in the world (Yao 2004). Unfortunately, the ecosystem degradation and loss in biodiversity caused by climate change are irreversible (VdePRda 2004). However, such changes in climate system are expected to continue into the future and beyond (IPCC 2007).

Soil temperature (ST), representing the thermal regime of the ground at a given location, is an indicator of climate change as its rapid response. Knowledge of ST trends in long

✉ Siqiong Luo
lsq@lzb.ac.cn

¹ Plateau Atmosphere and Environment Key Laboratory of Sichuan Province, School of Atmospheric Sciences, Chengdu University of Information Technology, Chengdu 610225, China
² Key Laboratory of Land Surface Process and Climate Change in Cold and Arid Regions, Northwest Institute of Eco-Environment and Resources, Chinese Academy of Sciences, Lanzhou 730000, China
³ Collaborative Innovation Center on Forecast and Evaluation of Meteorological Disasters, Nanjing University of Information Science & Technology, Nanjing 210044, China

time series through the soil profile is deemed as an effective approach to reflect the degree of climate change accurately (Yang et al. 2010a; Yang et al. 2010b). Recently, there have been numerous reports of ST variation associated with the climate change in various parts of the world, such as Alaska and Siberia (Oelke and Zhang 2004), Turkey (Yeşilirmak 2014), Canada (Qian et al. 2011), Russia (Zhang et al. 2001), and China (Wang et al. 2009; Wang et al. 2014b; Wu and Zhang 2008).

As “the roof of the world,” the Tibetan Plateau (TP) is characterized by its high elevations and complex topography. Studies have shown that the TP is particularly sensitive to climate warming impacts (Liu and Chen 2000; Wang et al. 2014a). Being higher than the surroundings, climate change on the TP could induce significant feedbacks through affecting the atmosphere circulation, and thus the Asia climate system even to global, owing to its unique mechanical and thermodynamic effects (Duan et al. 2011; Wu and Duan 2013). Characterized by the alpine climate, the annual air temperature (AT) is low which varies from 20 °C to no more than −6 °C through the southeast the northwest section. Owing to the cold and semi-arid climate features, one classical terrain features of the TP is the widespread permafrost or the seasonal frozen ground. The permafrost, covering an area of 1.73×10^6 km² (Yang et al. 2010a), occupies greater than two thirds area of the TP, while areal extent of seasonally frozen ground (including the active layer over permafrost) covers, on average, approximately all of the TP (Wu and Zhang 2008).

Studies have shown that the frozen ground of TP is relatively warm and thin compared with high latitude frozen ground in both North America and Russia sections, and thus is more sensitive to climate change (Cheng 1999; Luo et al. 2016). The freezing and thawing processes that occurred at the soil profile play an important role in determining the nature of land and atmosphere interactions (Guo et al. 2011). Based on observations, conclusions have been drawn that the heat exchange during soil thawing (freezing) is 3 (3.5) times more than that without phase change (Li et al. 2002). Observations on the TP also indicate the significant diurnal variation of ST resulted in a diurnal cycle of unfrozen water content at the surface (Guo et al. 2011). Numerical simulation results indicate that the freeze-thaw process is a buffer to the seasonal changes in soil and near-surface temperature and strengthens the energy exchange between the soil and the atmosphere (Chen et al. 2014). However, the time that the ground surface on the TP experienced diurnal freeze/thaw cycles was about 6 months (Yang et al. 2007). An increase of mean annual AT on the TP has resulted in extensive permafrost degradation. Discontinuous permafrost bodies and thawed nuclei have been widely detected (Wang et al. 2000). A large scale of permafrost tends to devolve into seasonal frozen ground,

sometimes even unfrozen soil, amplifying the climatic effect of freeze/thaw process of the TP, including the ecosystem functions and engineering projects. As a direct reflection of climate change as well as the situation of freeze-thaw on the TP, it is important to understand the spectrum of ST changes taken place, such as trends, variability, and spatial distribution, also the inducing factors of abrupt changes within the region from a climatic perspective.

The objective of this paper was to reveal the detailed factors related to the TP soil warming by examining the full spectrum of climate variables changes occurring. Five observed meteorological variables relevant to TP climate change were examined. The variables include the monthly soil temperature (ST) at depth of 0, 5, 10, 15, 20, 40, 80, 160, and 320 cm, respectively, mean air temperature (AT), precipitation (P), the annual maximum frozen depth (MFD) and snow cover depth (MSD), also the monthly observed frozen depth (FD) and snow cover depth (SD). Records from 1960 to 2014 were selected for this paper, which is the most comprehensive investigation and longest timeframe that has been applied thus far to the region.

2 Data and methods

2.1 Data

Monthly observations including ST at 0 to 320 cm, mean AT at 2 m above the surface, P, FD, and SD were obtained from 66 meteorological stations operated by the China Meteorological Data Sharing Service System. The annual MFD and MSD were obtained from the maximum monthly values while the annual P was obtained from the accumulation of monthly values. Professional meteorological technicians were applied in variables monitoring. The observation of ST from 0 to 40 cm underground were conducted four times per day (02:00, 08:00, 14:00, and 20:00, Beijing Time) and averaged as the daily mean, while once per day (14:00, Beijing Time) from 80 to 320 cm (CMA 2003). The values of FD were observed once per day (08:00, Beijing Time) using frozen soil apparatus when the surface ST was below 0 °C (CMA 2003; Luo et al. 2016). All values were obtained from the monthly means of daily values from 1960 to 2014, with the exception of P. The monthly P, however, was obtained from the monthly accumulation of daily values. The monthly data were then used to create seasonal and annual time series.

Although the qualities of the variables have been carefully controlled before releasing, some false and missing data are

obtained inevitable. In this study, the annual values of ST were retained if the readings were available for the whole 12 months of the year, while a missing value was assigned. The ST values of individual stations were only accepted while there were fully records of more than 30 years during the 55 years (1960–2014). Based on this criterion, 62 stations were selected for surface ST (0 cm) analysis, 49 and 17 for shallow (5–20 cm), and deep (40–320 cm) ST analyses, respectively (Table 1). Number of stations selected for AT, P, (M)FD, and (M)SD analyses are also listed in Table 1. Regional shallow and deep ST data were derived by simply averaging the data from 5 to 20 cm and 40 to 320 cm. Seasonal data, calculated from the monthly time series, were classified as spring (March–April–May, MAM), summer (June–July–August, JJA), autumn (September–October–November, SON), and winter (December–January–February, DJF) in this study.

Individual stations selected in this study are presented in Fig. 1. In terms of spatial distribution, these stations, mainly located on the northeast, interior, and southwest sections of the TP, are typically established close to densely inhabited areas. Depending on the ST at 3.2 m, Frauenfeld (Frauenfeld 2004) has previously classified the location as either permafrost or seasonally frozen ground. The individual location was deemed as seasonally frozen ground while the ST at 3.2 m is above zero, otherwise the permafrost. Based on this standard, the stations obtained in this study were classified as seasonally frozen ground.

2.2 Methods

The null hypothesis slopes of meteorological variables were investigated with a confidence level of 95 or 99% in this study by means of two non-parametric methods: the modified Mann–Kendall trend (MMK) (Hamed and Rao 1998; Zhang 2010) and Sen’s slope estimator (Gocic and Trajkovic 2013; Sen 1968). They are common methods that have been widely accepted for statistical diagnosis in modern climatic analysis studies (Luo et al. 2016; Silva et al. 2015; Yue et al. 2002).

Table 1 Number of meteorological stations selected for individual variables this study

ST			AT	P	(M)FD	(M)SD
Surface	Shallow	Deep				
62	49	17	62	62	53	61

2.2.1 The modified Mann–Kendall trend

The statistic S was calculated as the following:

$$s = \sum_{i=1}^{n-1} \sum_{j=i+1}^n \text{sgn}(x_j - x_i), \tag{1}$$

where n is the number of data points, x_i and x_j are ($j > i$) the data values in time series.

The sign function $\text{sgn}(x_j - x_i)$ was expressed as the following:

$$\text{sgn}(x_j - x_i) = \begin{cases} +1, & \text{if } x_j - x_i > 0 \\ 0, & \text{if } x_j - x_i = 0 \\ -1, & \text{if } x_j - x_i < 0 \end{cases} \tag{2}$$

In the Mann–Kendall trend method, the variance $\text{Var}(S)$ was calculated as the following:

$$\text{Var}(S) = \frac{n(n-1)(2n+5) - \sum_{i=1}^m t_i(t_i-1)(2t_i+5)}{18}, \tag{3}$$

where n is the number of data points, m is the number of tied groups, and t_i denotes the number of ties of extent i .

However, owing to the evidence for the existence of positive autocorrelation in the data ($n > 10$), this approach would increase the probability of detecting trends when actually none exist, and also non-detection of real trends in the data (Hamed and Rao 1998).

For the time series $X = \{x_1, x_2, \dots, x_n\}$, we need to acquire the stable series $\{y_i\}_{i=1}^n$ after removing the value of β :

$$y_i = x_i - \beta \times i. \tag{4}$$

where the trend estimator β based on the rank of series is the following:

$$\beta = \text{median} \frac{x_j - x_i}{j - i} \quad (1 \leq i < j \leq n). \tag{5}$$

The autocorrelation function $r(i)$ was calculated as the following:

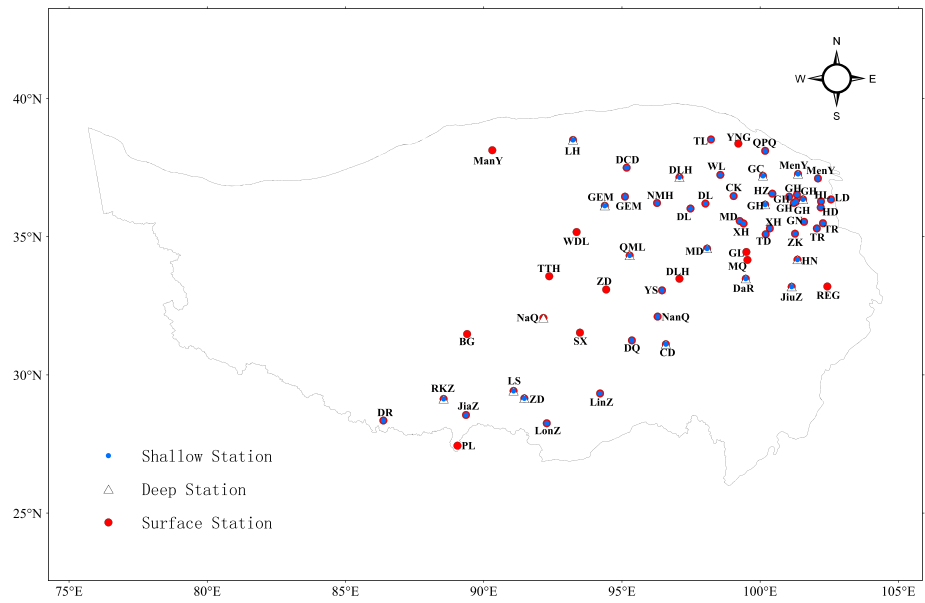
$$r(i) = \frac{\sum_{k=1}^{n-i} (R_k - R)(R_{k+i} - R)}{\sum_{k=1}^n (R_k - R)^2}. \tag{6}$$

where R_i is the rank of $\{y_i\}_{i=1}^n$ and R is the mean of R_i .

Furthermore, a correction for the autocorrelation in the data was the following:

$$\eta = 1 + \frac{2}{n(n-1)(n-2)} \times \sum_{i=1}^{n-1} (n-i)(n-i-1)(n-i-2)r(i). \tag{7}$$

Fig. 1 The map shows the locations and names of meteorological stations located within the TP. Red dots on the map represent stations with satisfactory observation data at surface (0 cm). Similarly, blue dots represent that at shallow layer (5–20 cm) and the triangles represent that at deep layer (40–320 cm)



Station	Station	Station	Station	Station	Station	Station	Station
ManY	MangYa	LH	LengHu	TL	TuoLe	YNG	YeNiugou
QPQ	QiaPuqia	DCD	DaChadan	DLH	DeLinha	WL	WuLan
GC	GangCha	MenY	MengYuan	GEM	GeErmu	NMH	NuoMuhong
DL	DuLan	GH	GongHe	CK	ChaKa	HZ	HuangZhong
HL	HuaLong	LD	LeDu	TR	TongRen	XH	XingHai
WDL	WuDaoliang	QML	QuMalai	MD	MaDuo	TD	TongDe
GN	GuiNan	ZK	ZeKu	DaR	DaRi	MQ	MaQin
GL	GuoLuo	HN	HeNan	TTH	TuoTuohe	ZD	ZaDuo
YS	YuShu	HD	HaiDong	JiuZ	JiuZhi	REG	RuoErgai
NaQ	NaQu	SX	SuoXian	NanQ	NangQian	BG	BanGe
DQ	DingQin	CD	ChangDu	RKZ	RiKeze	LS	LaSa
LinZ	LinZhi	ZD	ZeDang	LonZ	LongZi	JiaZ	JiangZi
PL	PaLi	DR	DingRi				

Based on η , we can calculate the modified variance $Var^*(S)$ in the MMK trend method as the following:

$$Var^*(S) = \eta \times Var(S). \tag{8}$$

Also, the standard normal test statistic $Z_s (n > 10)$ was calculated in MMK as the following:

$$Z_s = \begin{cases} \frac{S-1}{\sqrt{Var^*(S)}}, & \text{if } S > 0 \\ 0, & \text{if } S = 0 \\ \frac{S+1}{\sqrt{Var^*(S)}}, & \text{if } S < 0 \end{cases} \tag{9}$$

Positive values of Z_s indicate increasing trends while the negative values of Z_s show decreasing trends. The specific α significance level was chosen to test the trends of MMK. The null hypothesis was rejected while $|Z_s| > Z_{1-\alpha/2}$ and a significant trend was present in the data series. The value of $Z_{1-\alpha/2}$ was obtained from the standard normal distribution table. Significance levels of $\alpha = 0.01$ and $\alpha = 0.05$ were used in this study. The null hypothesis of “no trend” is rejected if $|Z_s| > 1.96$ at the 5% significance level and $|Z_s| > 2.576$ at the 1% significance level (Gocic and Trajkovic 2013).

2.2.2 Sen’s slope estimator

For the sample of N pairs of data, the non-parametric procedure for estimating the slope was the following:

$$Q_i = \frac{x_j - x_k}{j - k} \text{ for } i = 1, \dots, N, \tag{10}$$

where x_j and x_k are the data values at times of $j, k (j > k)$.

If there was only one datum in each time period:

$$N = \frac{n(n-1)}{2}, \tag{11}$$

where n is the number of time periods.

Otherwise,

$$N < \frac{n(n-1)}{2}, \tag{12}$$

where n is the total number of observations.

The N values of Q_i were ranked from smallest to largest. The Sen’s slope estimator (essentially the median of the slope) was calculated as the following:

$$Q_{med} = \begin{cases} Q_{[(N+1)/2]}, & N \text{ is odd} \\ \frac{Q_{[N/2]} + Q_{[(N+2)/2]}}{2}, & N \text{ is even} \end{cases} \tag{13}$$

The sign of Q_{med} reflects the data trend; its value indicates the slope of the trend (Sen 1968).

In addition, the confidence interval (C_α) of Q_{med} at specific probability should be obtained to determine the significance level of the trend:

$$C_\alpha = Z_{1-\alpha/2} \sqrt{Var^*(S)}, \tag{14}$$

where $Var^*(S)$ is calculated from Eq. (8) and $Z_{1-\alpha/2}$ is obtained from the standard normal distribution table. The confidence interval was computed at two significance levels ($\alpha = 0.01, \alpha = 0.05$) in this study.

Based on Gilbert (Gilbert 1987), $M_1 = \frac{N-C_\alpha}{2}$ and $M_2 = \frac{N+C_\alpha}{2}$ were calculated. As the lower and upper limits of the confidence interval, Q_{min} and Q_{max} are the M_1 th largest and the $(M_2 + 1)$ th largest of the N ordered slope estimates, respectively (Gocic and Trajkovic 2013). If the two limits (Q_{min}, Q_{max}) have a similar sign, the slope Q_{med} can be considered statistically significant.

3 Results

3.1 Statistical information of meteorological variables in annual and seasonal time series

Statistical information including means, standard deviations, and trends in annual and seasonal ST, AT, P, FD, and SD, also the MFD and MSD, are listed in Table 2. Figure 2 illustrates trends in ST at surface, shallow, and deep layer from individual meteorological stations. On the annual scale shown in Table 2, the mean TP ST were 6.12, 7.09, and 6.81 °C at surface, shallow, and deep layers, respectively. However, the annual mean TP AT was just 2.51 °C, which far less than the ST. More than half of meteorological stations measured AT below zero. Moreover, regional surface ST standard deviation (0.91) was higher than that of AT (0.76), indicating larger inter-annual surface ST variation within the area. In terms of seasonal scale, major variation was found for winter (1.33), with the average increasing trend of 0.57 °C/decade at the 99% significant level. The ST variations at shallow were also significant in spring and summer, with significant (99%) trends of 0.43 and 0.41 °C/decade. However, the maximum magnitude of soil warming occurred in summer at deep, with trend of 0.58 °C/decade. Correspondingly, annual and seasonal trends in AT near the surface were lower than those for surface ST on average, implying that, in general, the soil on the TP is highly sensitive and respond quickly to the climate change applied upon it. Trend in AT in winter is higher than those in other seasons indicate the increase in winter AT contributed more to increases in AT in the TP. In terms of spatial distribution, the significant ST warming (Fig. 2) was common for all meteorological stations in the TP, with the exception of

Table 2 Statistical information of seasonal and annual meteorological time series in the entire TP from 1960 to 2014

	ST(surface)			ST(shallow)			ST(deep)		
	μ (°C)	σ (°C)	Trend (°C/decade)	μ (°C)	σ (°C)	Trend (°C/decade)	μ (°C)	σ (°C)	Trend (°C/decade)
Spring	8.15	1.15	0.47**	7.56	1.00	0.43**	4.68	0.72	0.37**
Summer	17.80	1.15	0.37**	17.13	1.02	0.41**	11.69	0.87	0.58**
Autumn	5.52	1.05	0.46**	7.68	0.78	0.33**	9.66	0.64	0.38**
Winter	-6.99	1.33	0.57**	-4.07	0.83	0.29**	1.93	0.54	0.16**
Annual	6.12	0.91	0.47**	7.09	0.70	0.36**	6.81	0.60	0.37**
	AT			P			FD		
	μ (°C)	σ (°C)	Trend (°C/decade)	μ (mm)	σ (mm)	Trend (mm/decade)	μ (cm)	σ (cm)	Trend (cm/decade)
Spring	3.44	0.86	0.26**	63.89	23.44	2.79	73.06	20.69	-6.47**
Summer	12.46	0.81	0.29**	233.69	55.09	3.23	-	-	-
Autumn	2.58	0.92	0.35**	78.77	27.61	0.66	-	-	-
Winter	-8.43	1.31	0.50**	6.64	4.15	0.48	95.61	13.10	-3.61*
Annual	2.51	0.76	0.35**	382.75	70.63	7.36	48.03	9.26	-3.78**
	MFD			SD			MSD		
	μ (cm)	σ (cm)	Trend (cm/decade)	μ (cm)	σ (cm)	Trend (cm/decade)	μ (cm)	σ (cm)	Trend (cm/decade)
Spring	-	-	-	2.72	1.49	-0.06	-	-	-
Summer	-	-	-	-	-	-	-	-	-
Autumn	-	-	-	-	-	-	-	-	-
Winter	-	-	-	1.79	1.06	0.03	-	-	-
Annual	117.51	17.98	-5.58**	1.61	0.64	-0.05	6.24	3.22	-0.07

μ mean, σ standard deviation

*Denotes trends statistically significant at $\alpha = 0.05$

**Denotes trends statistically significant at $\alpha = 0.01$

significant common downward trends of Lenghu, Menyuan, Geermu, Xining, and Maduo in winter at deep.

P decreased from the southeast to the northwest in the TP area owing to the soaring mountains that blocked moisture entering (Liang et al. 2013). The proportion of summer P in annual P exceeded 60% for all meteorological stations in the TP. The spring P was the same order of magnitude as the autumn one, with the average values of 63.89 and 78.77 mm, respectively. Regional P was scarce in winter in the area compared to other seasons, with the average value of 6.64 mm. In general, the mean annual P during the past decades was increasing with trend of 7.36 mm/decade, however, varied at individual season within the TP. The increasing P occurred in the area mainly focused on spring and summer, with trends of 2.79 and 3.23 mm/decade, respectively. Major inter-annual variation of P in the TP occurred in summer based on the statistical information in Table 2. However, the increasing variation of spring P was also considerable owing to the obviously lower mean value (68.39 mm) compared to summer (233.69 mm). The individual stations with significant increasing P were mainly located in the northeastern and interior sections of the TP (Fig. 3a), so as the winter P (Fig. 3d). The

stations with significant increasing P were mainly focused on the northeastern TP (Fig. 3b). Increasing or decreasing trend of P in autumn was not as significant as others, excepting the Jiuzhi and Dulan decreasing with rates of 7.21 and 4 mm/decade at 95% significant level and Yiwu increasing with rate of 1.96 mm/decade at 99% significant level.

Mean annual FD was 48.03 cm for the TP, ranging from 2 to 183.05 cm between individual meteorological stations (not shown in this paper). Statistic results of FD in spring and winter which need to focus on were listed in Table 2. Based on the statistical results, FD for the area has shown greater inter-annual variation (20.69) and significant decreasing trend (6.47 cm/decade) in spring at 99% significant level during the past decades. Relative milder variation of FD was detected in winter with less significant degree (95%). Average decreasing trends of FD among meteorological stations are 3.61 cm/decade in winter and almost half of the trend detected in spring. This might closely relate to the extent of ST warming at deep layer. It has been widely accepted that permafrost or seasonal frozen ground (soil or rock) are classified with criterion of the duration of ST remains at or below 0 °C (Cheng 1999; Frauenfeld 2004; Muller and SiemonWilliam 1947; Zhao

Fig. 2 Spatial distributions of annual (a1–a3) and seasonal (b1–e3) temporal trends for ST at surface (the first column), shallow (the second column), and deep layer (the last column) from 1960 to 2014, respectively. Upward and downward triangles show positive and negative trends, respectively. Solid triangles indicate trends significant at the 5% level

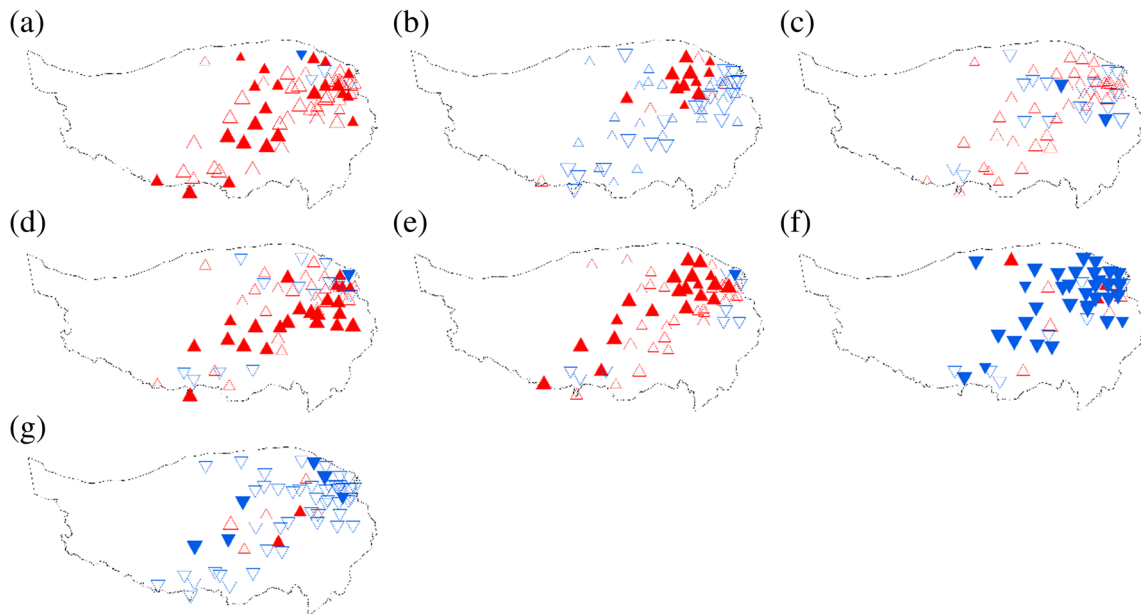
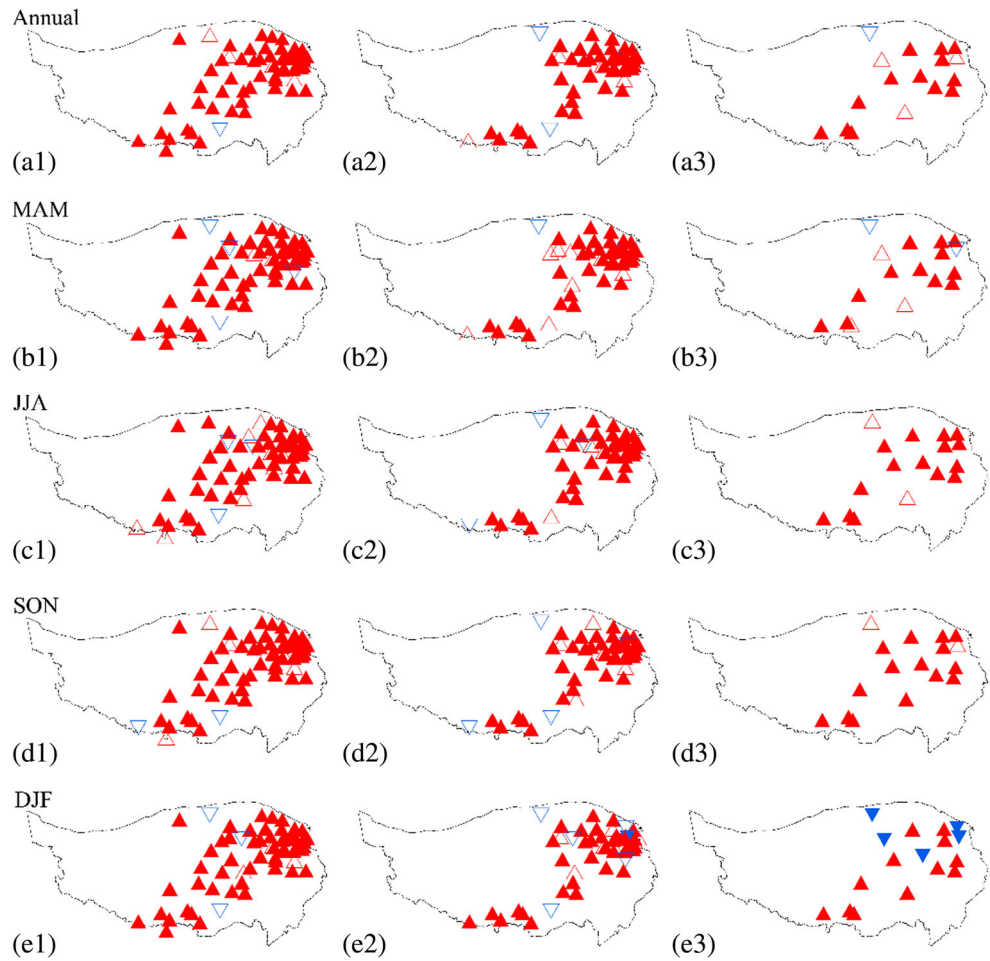


Fig. 3 Same as Fig. 2, but for seasonal and annual temporal trends in mean P **a** spring (MAM), **b** summer (JJA), **c** autumn (SON), **d** winter

(DJF), and **e** annual, MFD (**f**) and MSD (**g**). The size of triangles indicated values of variable trends

et al. 2004). The 0 °C isotherm throughout the soil profile was confirmed to find the monthly depth of the freezing layer. The maximum depth was obtained from the monthly values for each year in our study. Regionally, the mean annual FD mentioned above (48.03 cm) for the TP exceeds 40 cm, implying that, in general, FDs discussed at individual stations in our study mainly reflected the ST conditions at deep layer from 1960 to 2104. As a result, more drastic ST warming in spring has more salient influences on FD decreasing compared to winter. Mean annual MFD reached 117.51 cm at these meteorological stations mainly situated in the northern and eastern sections of the TP where annual decreasing trend is significant at 5.58 cm/decade (99%). Figure 3e illustrates trends in MFD from individual meteorological stations. The stations that showed significant negative trends (99%) at most meteorological stations, with only a few stations showing significant increasing trends ($\alpha = 0.05$ or $\alpha = 0.01$). Trends in MFDs at Lenghu, Linzhi, were the reverse for the other significant ones. MFD at these two stations were increasing with significant trends ($\alpha = 0.01$) of 12.17, 1.04 cm/decade, respectively.

As shown in Table 1, mean annual TP SD was 1.61 cm, ranging from 0.12 to 4.01 cm depending on individual stations (not shown). Variations in annual and season SD among the meteorological stations were lower compared to FD (Table 2). Only a few meteorological stations are showing significant trends ($\alpha = 0.05$ or $\alpha = 0.01$). An insignificant decreasing trend of 0.05 cm/decade for annual SD was determined for the TP between 1960 and 2014, corresponding to the increase in annual P that took place in the past decades. Dramatic warming condition of the near surface atmosphere over the TP might be responsible for the warmer, wetter period of the most TP. Regional mean SD standard deviation was high in spring (1.49), corresponding to the large inter-annual AT, P variations (spring) within the area. Although trends for the annual or season series on a regional scale were low, individual stations did exhibit variable characteristics. Spatial pattern of trends for MSD at individual stations varied greatly. The stations showed significant negative trends were located in the northeast section, also the interior TP. However, Yushu and Geermu exhibited low but significant increasing trends ($\alpha = 0.01$) (Fig. 3f). Taking the entire TP into account, MSD decreased at 0.07 cm/decade (annual series).

Regionally, no uniform pattern was found for trends in all five variables in terms of spatial distribution. The majority of stations showed significant positive ST (surface, shallow and deep), AT trends, and significant negative (M)FD trends; whereas, fewer stations showed significant trends for P and (M)SD. In general consideration, annual P increased from southwest to northeast section throughout the TP, with the exception of Huzhu with significant decreasing trend in the northeastern part (Fig. 3e). Annual MSD appeared to have a high spatial variability. Significant trends were detected at eight stations, where decreasing trends were measured at six stations out of the eight. Larger trends, decreasing or

increasing, mainly appeared in the central and northeastern sections of the TP (Fig. 3g).

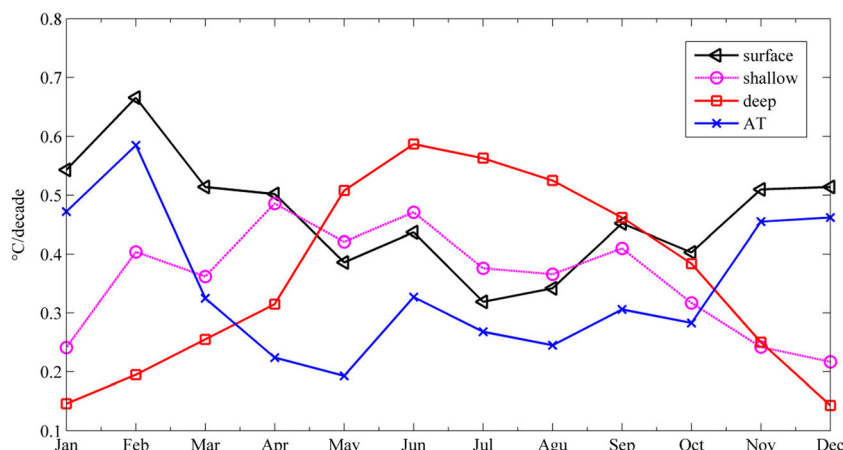
3.2 Trends of ST in the monthly time series

Inter-monthly variation of trends in ST at each layer is provided in Fig. 4. Means of surface, shallow, and deep ST increased from 1960 to 2014, with sharp increases occurring in January, January, and April, implying that the warming occurred in surface might take some time to the deep. Value of surface soil warming was extremely high (0.67 °C/decade) in February and decreased thereafter. After the late July, the magnitude of soil warming started to rise sharply once again. Being susceptible to random weather processes, the rapid surface soil warming occurred from January to February could also be associated with the freezing process of seasonal frozen ground as well as snow accumulation. Numerical simulation results have indicated that as a buffer to the seasonal changes in soil and near-surface temperatures, the freeze (thaw) process tends to release (absorb) phase energy, thus retards the cooling (heating) effect of AT on soil (Chen et al. 2014). The freezing process occurred in surface soil during this period tended to release amount of latent heat of phase change to around, thus accelerating the warming process logically. In addition, the snow accumulation accompanied with the growing SD in winter (Table 2) affects the near surface ST because of high albedo, insulation effects.

Magnitudes of warming trends fluctuated up and down at shallow soil from 1960 to 2014. Taking the entire variation trends into account, the warming trends increased from January to June and decreased thereafter. Regionally, there exist twice warming jumps in shallow soil that occurred in January and March, respectively. Similar to the surface, the ST in shallow also gently increased from February to March on average. This might also be induced by the thawing (energy absorbing) process of frozen ground as well as the snowmelting that occurred in these two layers during this period. Maximum warming trend occurred at shallow reached 0.50 °C/decade in April and appeared to have undergone decreasing trend of soil warming in duration. In contrast, the surface ST began to warm sharply in October and this might be related to the significant near surface air warming in winter.

Warming trends in deep increased from January to June and decreased in the last year. These were the reverse for the variation of surface warming trends. A sharp warming in deep soil occurred in April, and reached up to 0.61 °C/decade in June. Whereafter, the warming trends decreased slightly in July and August. Also, in this layer, the soil showed apparent lower increasing trends during October, corresponding to the steady increasing warming trends in surface that occurred in this period. The soil profile

Fig. 4 Trends estimated from monthly ST (surface, shallow, and deep) and AT



appeared to have undergone energy transmission from deep to surface. The freezing process occurred in advance in surface tended to absorb energy from deep as well as the atmosphere near the surface.

3.3 Relationship between ST and surface AT

AT most meteorological individual stations, annual and seasonal AT showed increasing trends, being significant at 99% (or 95%) confidence level. A significant warming trend of 0.35 °C/decade ($\alpha = 0.01$) was determined for the TP, corresponding to the increase in surface ST (0.47 °C/decade, $\alpha = 0.01$). In terms of seasonal variation, the sharp warming in AT occurred in winter with the maximum value of 0.50 °C/decade (Table 1), corresponding to the sharp soil warming in surface (0.57 °C/decade). Sizable increases in AT associated with the surface ST implying the dominate effect of climate warming on surface ST. Considerable air warming in winter also indicated the significant increase in minimum AT over the TP throughout 1960–2014. The air warming is mainly dominated by the winter warming in the past decades.

All ST variables averages for the past decades were compared with AT (Fig. 4) throughout the study period to identify the relationship between ST and AT under the warming background taking place in the TP. Monthly trends in STs and AT were also listed in Table 3. Majority of the meteorological individual stations did exhibit air warming characteristics. The air over the stations showed sharp increasing warming trend in November and reached up to the maximum value of 0.59 °C/decade in February. In the months which followed, the warming trends fluctuated up and down, ranging from 0.19 to 0.33 °C/decade between individual months. Figure 4 illustrates the close relationship between warming trends of surface ST and AT. Moreover, the warming trends occurred in surface ST exceed the AT throughout the period, which confirms that the ST in the TP is highly sensitive and responded quickly to the climate warming as described in previous section.

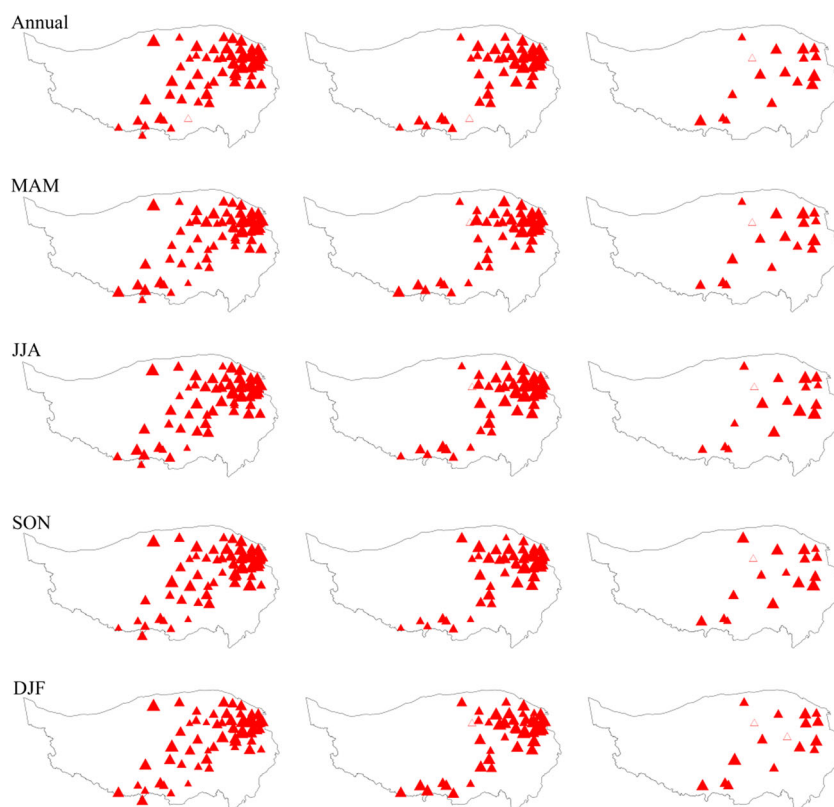
Other than the strikingly good relationship in warming trends between AT and surface ST, trends in shallow and deep STs showed no apparent relationships with AT over the 55-year study period. Trends of soil warming in shallow (0.36 °C/decade) started to outpace those in AT in March (0.33 °C/decade), and continue until the late October. Whereafter, the warming trend of AT increased sizably (0.46 °C/decade) was nearly twice that of November in shallow soil (0.24 °C/decade). On the other hand, the periodical variations detected for the trends in deep ST appeared to be the reverse for the AT. The deep ST warmed greatly from mid-March to the early October, with maximum value of 0.59 °C/decade during this period. The trends in AT, analogously, fluctuated up and down but with obviously limited magnitudes (0.33 °C/decade) during this period. However, the warming trends in deep ST and AT tended to move in the opposite direction in the rest of the year. These variation patterns are similar to those of surface and deep STs.

Spatial patterns of correlations between annual and seasonal soil and air temperatures varied slightly (Fig. 5). Majority of

Table 3 Warming trends (°C/decade) of meteorological variables in monthly time series in the entire TP from 1960 to 2014

Month	ST(surface)	ST(shallow)	ST(deep)	AT
1	0.54	0.24	0.15	0.47
2	0.67	0.40	0.20	0.59
3	0.51	0.36	0.26	0.33
4	0.50	0.49	0.32	0.22
5	0.39	0.42	0.51	0.19
6	0.44	0.47	0.59	0.33
7	0.32	0.38	0.56	0.27
8	0.34	0.37	0.53	0.25
9	0.45	0.41	0.46	0.31
10	0.40	0.32	0.38	0.28
11	0.51	0.24	0.25	0.46
12	0.51	0.22	0.14	0.46

Fig. 5 Same as Fig. 2, but for correlations between ST and AT from 1960 to 2014. Upward (downward) triangles show positive (negative) correlations. Red triangles represent the correlation relationships were statistically significant ($\alpha = 0.01$ or $\alpha = 0.05$). Open triangles indicate no significant correlation relationships. Sizes of triangles represent the degrees of correlations between the variables



the meteorological stations did exhibit significant ($\alpha = 0.01$ or $\alpha = 0.05$) positive correlations between ST and AT; whereas, few stations showed insignificant positive correlations for the variables. In the marginal area of the TP in Fig. 5 (the first column), the correlation values between surface ST and AT were greater than those in the interior section. Generally, the correlation values were greater in winter, also confirming the perfect close relationships between surface ST and AT. Meanwhile, the strong AT warming areas, which coincide with the significant shallow ST warming, mostly lie in the northeastern part of the TP area. Warming trends in deep soil appeared to have undergone closer correlation relationship with climate warming in the mid-eastern section of TP in spring and summer. However, in winter, the strong correlation relationships tended to concentrate on the southwest regions.

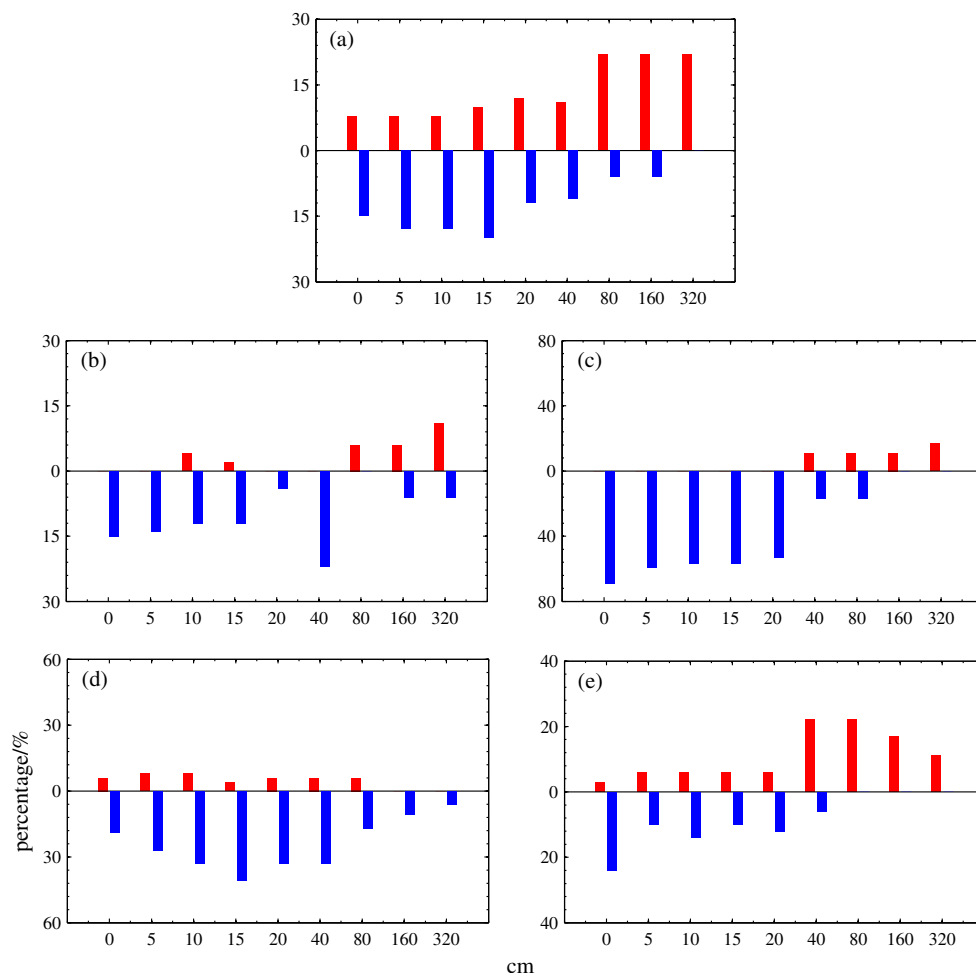
3.4 Relationship between ST and other climate variables

It is useful to examine the relationships between ST and P, FD and SD because of their various features of which may be used as indicators to account for the ground thermal regime as well as parameters for future climate prediction in the TP. The proportions of meteorological stations with significant correlation relationships between ST and P were provided in Fig. 6. In general, over land, relationship between ST and P was characterized by a negative correlation, as dry conditions favor more

sunshine and less evaporative cooling, while wet summers are cool (Trenberth and Shea 2005). For example, a significant negative correlation relationship has been detected widely in the meteorological stations in this study on annual or seasonal time series (Fig. 6). However, being located as a unique geographical unit, the TP exhibited unique characteristics. Not all stations exhibited the same direction in correlation between ST and P. Significant positive correlations relationships between the two variables have also been detected in individual stations (Fig. 6). Moreover, the positive direction dominated the correlation relationship between annual ST and P in deep layer from 80 to 320 cm (Fig. 6a). In terms of seasonal temporal series, more frequent positive relationships between surface or shallow ST and P were detected in autumn and winter. Significant positive correlation relationship between the two meteorological variables was observed more often in deep soil in winter. Stations with significant positive relationship occupy more than one-fifth (23.5%) of the total (Fig. 6e). The warming trend in deep soil began to accelerate widely in winter and yielded a perfect positive correlation relationship with increased P. The correlation relationship between the surface or shallow ST and P was the reserve for that in deep in summer (Fig. 6c). Significant correlations between surface (shallow) ST and P were detected at 43 (28) stations out of the 62 (49), where the negative ones occupied all of the significant ones.

The P feedback mechanisms occurred in spring and thermal insulation effect of snow cover that occurred in winter made

Fig. 6 The proportions of stations with significant correlation relationship (at 95% significant level) between ST and P in **a** annual, **b** MAM, **c** JJA, **d** SON, and **e** DJF temporal series. Red (blue) bars represent proportions of stations with significant positive (negative) correlations



these correlation relationships complicated. Furthermore, the remarkable permafrost shrinkage, which tends to devolve into the seasonal frozen ground or even to unfrozen soil, are determined to be responsible for the results. As previously stated, the “buffer” effect of freeze (thaw) process in frozen ground accompanies energy releasing (absorbing) throughout the soil should be react on the ST. Previous studies have indicated the energy throughout the soil tends to transmit from the deep to the surface in autumn (winter) and was the reverse in spring (summer). Relative warmer P loaded on the frozen ground tend to change the thermal regime regionally. The frozen soil in upper layer appeared to have undergone shorten complete frozen duration in winter and a certain amount of extra energy was needed for the ice melting. The surface ground, however, tends to absorb greater amount of energy from the deep soil, also the surroundings by this time. The increased P load, making greater energy transmission and ST increasing regionally. Correspondingly, the increased P load tended to have an inhibitory effect on the surface or shallow ST increase in summer. Also, the thawing process, induced by the increased P during the summer in the frozen soil, was supposed to absorb energy from surroundings. The deep ST (from 40 to 320 cm), however, yielded positive correlation

relationship with P during this period. The sharp ST warming occurred in deep during summer agreed well with the increased P.

As expected, FDs have a consistent influence on STs, showing a significant negative correlation (not presented). The snow cover, which influences the ground thermal regime as well as the near surface air, occupies an irreplaceable position in land-atmosphere interaction studies (Goodrich 1982; Ming et al. 2013; Qian et al. 2011). For example, the insulation effect of snow cover on the ground normally results in higher ST in winter and lower ST in spring and autumn (Qian et al. 2011). Consequently, the decreasing or increasing trend of SD in the TP might be crucial to the ST variation, also the near surface AT, even to the regional or global atmosphere circulation. The proportions of stations with significant correlations between SD and ST in spring and winter were illustrated in Fig. 7. Correlation patterns of the two variables varied greatly in seasons. It is apparent that the decreased SD (0.06 cm/decade, Table 2) in spring was closely related to the increased ST, especially in surface and shallow layers (Fig. 7a). Decreasing SD in spring means decreasing surface albedos, resulting in the decreased energy loss in land-surface energy budget. Correlations between deep ST and

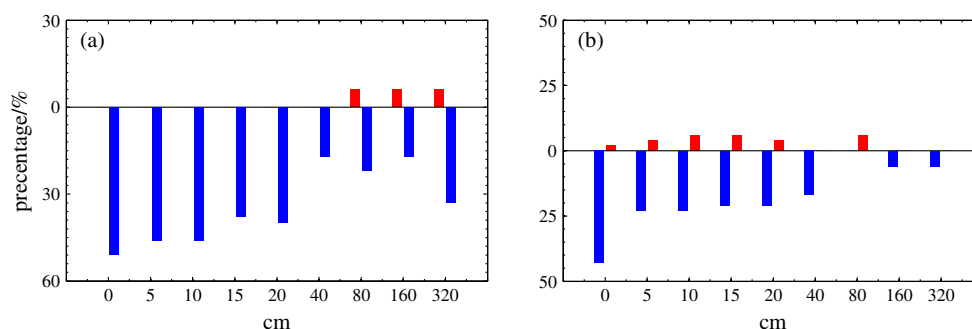


Fig. 7 Same as Fig. 6, but for the ST and SD in **a** MAM and **b** DJF

SD were also dominated by negative relationship, with the exception of Geermu. Correlations, however, showed positive values between the deep ST (80 to 320 cm) and SD in Geermu, being statistically significant at a 95 or 99% confidence level. An insignificant trend of $0.06\text{ }^{\circ}\text{C}/\text{decade}$ determined for the deep ST in this station was well corresponding to the slightly increasing SD. Stations showed weaker correlations in winter between ST and SD (Fig. 7b). The stations selected in this study exhibited a small increasing SD trend in winter on average ($0.03\text{ cm}/\text{decade}$, Table 2), accompanied with significant ST warming. However, the insulation effect of snow cover on ST may not always occur at a particular location in the TP. A low proportion of stations showed significant positive correlation, including Geermu, Delinha, and Dari. These positive correlations were mainly determined in surface and shallow layers. Nevertheless, correlations between ST and SD with significant levels ($\alpha = 0.01$ or $\alpha = 0.05$) were determined as negative widely. Being different from other regions (Goodrich 1982; Ming et al. 2013; Qian et al. 2011; Qin et al. 2006), the averaged slightly increasing SD trends in winter had an inhibitory effect on the ST increase in the TP although the soil underwent significant warming in the area during 1960–2014. The low average SD (1.61 cm, Table 2) in the TP might be responsible to the extremely weak insulation effect on ST. On the other hand, the significant warming trends of AT accompanied with the ST tended to induce the snowmelting regionally, following the energy absorption and cooling process in upper soil layer.

4 Conclusions

Temporal variations in ST (0 to 320 cm), AT, P, (M)FD, and (M)SD in the TP were analyzed by modified MK and Sen's slop estimator methods from 1960 to 2104. Conclusions drawn from the analysis are listed as follows:

Significant warming trends of soil have been detected in the TP across the 55 years. Rates of increase were $0.47\text{ }^{\circ}\text{C}/\text{decade}$ for surface (0 cm), $0.36\text{ }^{\circ}\text{C}/\text{decade}$ for shallow (0–20 cm), and $0.37\text{ }^{\circ}\text{C}/\text{decade}$ for deep (40–320 cm). The majority of individual meteorological stations did exhibited a sharp increasing trend in surface soil in winter; whereas, STs

increases in the spring and summer were more evident in shallow and deep layers than in the surface.

AT also increased significantly with an annual trend of $0.35\text{ }^{\circ}\text{C}/\text{decade}$ during 1960 to 2014. There exists a clear effect of AT warming on ST increases, especially on the surface soils. At most of the meteorological stations, the significant positive correlation relationships between ST and AT were determined as widely as the area.

P amounts increased over the past years at most of the individual stations. The trend of P was determined as $7.36\text{ mm}/\text{decade}$ on annual temporal series, but not obviously so. The correlation relationships between ST and P varied greatly based on individual locations owing to the P feedback mechanisms that occurred in spring and thermal insulation effect of snow that occurred in winter. Moreover, the increased P load might enhance the energy transfer throughout the soil as well as the surroundings.

SD decreased and increased slightly in spring and winter, respectively. The decreasing trend of SD was determined as $0.05\text{ cm}/\text{decade}$ on annual scale. The insulating effect of snow cover on the ST is weak. Correlations between ST and SD in the area was determined as negative at most of the individual stations owing to the decreased loss in the energy budget.

The combined effects of AT warming, P increasing, and SD and FD decreasing in the TP have induced the significant ST warming regionally, and this warming trend was expected to be continue in the foreseeable future.

Acknowledgements We are very grateful for the reviewers and the editor for constructive recommendations and advice.

Funding information This work was supported by the National Natural Science Foundation of China, grants 91537104, 41375077, 41775016, and 91537214. This work was also supported by the Opening Fund of Key Laboratory for Land Surface Process and Climate Change in Cold and Arid Regions, Chinese Academy of Sciences. Observation data on the TP were provided by the China Meteorological Data Sharing Service System.

Open Access This article is distributed under the terms of the Creative Commons Attribution 4.0 International License (<http://creativecommons.org/licenses/by/4.0/>), which permits unrestricted use, distribution, and reproduction in any medium, provided you give appropriate credit to the original author(s) and the source, provide a link to the Creative Commons license, and indicate if changes were made.

References

- Chen B, Luo S, Lü S (2014) Effects of the soil freeze-thaw process on the regional climate of the Qinghai-Tibet Plateau. *Clim Res* 59(3):243–257
- Cheng G (1999) Glaciology and geocryology of China during the past 40 years: progress and prospects. *J Glaciol Geocryol* 21(4):289–309
- CMA (2003) Specifications for surface meteorological observation. China Meteorological Press Beijing, China
- Duan A, Li F, Wang M, Wu G (2011) Persistent weakening trend in the spring sensible heat source over the Tibetan Plateau and its impact on the Asian summer monsoon. *J Clim* 24(21):5671–5682. <https://doi.org/10.1175/JCLI-D-11-00052.1>
- Frauenfeld OW (2004) Interdecadal changes in seasonal freeze and thaw depths in Russia. *J Geophys Res* 109(D5). <https://doi.org/10.1029/2003JD004245>
- Gilbert RO (1987) Statistical methods for environmental pollution monitoring
- Gocic M, Trajkovic S (2013) Analysis of changes in meteorological variables using Mann-Kendall and Sen's slope estimator statistical tests in Serbia. *Glob Planet Chang* 100:172–182. <https://doi.org/10.1016/j.gloplacha.2012.10.014>
- Goodrich LE (1982) The influence of snow cover on the ground thermal regime. *CaGeJ* 19(4):421–432
- Guo D, Yang M, Wang H (2011) Characteristics of land surface heat and water exchange under different soil freeze/thaw conditions over the central Tibetan Plateau. *Hydrol Process* 25(16):2531–2541. <https://doi.org/10.1002/hyp.8025>
- Hamed KH, Rao AR (1998) A modified Mann-Kendall trend test for autocorrelated data. *JHyd* (204):182–196
- Li S, Nan Z, Zhao L (2002) Impact of soil freezing and thawing process on thermal exchange between atmosphere and ground surface. *J Glaciol Geocryol* 24(5):506–511
- Liang L, Li L, Liu C, Cuo L (2013) Climate change in the Tibetan Plateau three rivers source region: 1960–2009. *IJCLI* 33(13):2900–2916
- Liu X, Chen B (2000) Climatic warming in the Tibetan Plateau during recent decades. *IJCLI* 20:1729–1742
- Luo S, Fang X, Lyu S, Ma D, Chang Y, Song M, Chen H (2016) Frozen ground temperature trends associated with climate change in the Tibetan Plateau three river source region from 1980 to 2014. *Clim Res* 67(3):241–255. <https://doi.org/10.3354/cr01371>
- Mackay A. Intergovernmental Panel on Climate Change (IPCC) (2007) Climate change 2007: impacts, adaptation and vulnerability. Contribution of Working Group II to the Fourth Assessment Report of the IPCC. Cambridge University Press, Cambridge, UK[J]. *Journal of Environmental Quality*, 2008, 37(6):2407
- Ming H, Zhihui L, Kai C, Rongjun W, Wenna Z (2013) Characteristics of soil temperature analysis under the influence of snow cover in the ablation period of seasonal frozen soil. *Research of Soil and Water Conservation* 20(3):39–43
- Muller, SiemonWilliam (1947) Permafrost or permanently frozen ground and related engineering problems. J.W.Edwards, Inc
- Niu G-Y, Yang Z-L (2007) An observation-based formulation of snow cover fraction and its evaluation over large North American river basins. *J Geophys Res* 112(D21). <https://doi.org/10.1029/2007JD008674>
- Oelke C, Zhang T (2004) A model study of circum-Arctic soil temperatures. *Permafrost Periglac Process* 15(2):103–121. <https://doi.org/10.1002/ppp.485>
- Qian B, Gregorich EG, Gameda S, Hopkins DW, Wang XL (2011) Observed soil temperature trends associated with climate change in Canada. *J Geophys Res* 116(D2). <https://doi.org/10.1029/2010JD015012>
- Qin D, Liu S, Li P (2006) Snow cover distribution, variability, and response to climate change in Western China. *J Clim* 19(9):1820–1833
- Sen PK (1968) Estimates of the regression coefficient based on Kendall's au. *J Am Stat Assoc* 63(324):1379–1389. <https://doi.org/10.1080/01621459.1968.10480934>
- Silva RMD, Santos CAG, Moreira M, Corte-Real J, Silva VCL, Medeiros IC (2015) Rainfall and river flow trends using Mann-Kendall and Sen's slope estimator statistical tests in the Cobre River basin. *Nat Hazards* 77(2):1205–1221. <https://doi.org/10.1007/s11069-015-1644-7>
- Trenberth KE, Shea DJ (2005) Relationships between precipitation and surface temperature. *Geophys Res Lett* 32(14):129–142
- VdePRda S (2004) On climate variability in northeast of Brazil. *J Arid Environ* 58(4):575–596
- Wang G, Hu H, Li T (2009) The influence of freeze-thaw cycles of active soil layer on surface runoff in a permafrost watershed. *JHyd* 375(3–4):438–449
- Wang S, Jin H, Li S, Zhao L (2000) Permafrost degradation on the Qinghai-Tibet Plateau and its environmental impacts. *Permafrost Periglac Process* 11(1):43–53
- Wang X, Yang M, Liang X, Pang G, Wan G, Chen X, Luo X (2014a) The dramatic climate warming in the Qaidam Basin, northeastern Tibetan Plateau, during 1961–2010. *IJCLI* 34(5):1524–1537
- Wang Y, Chen W, Zhang J, Nath D (2014b) Relationship between soil temperature in may over Northwest China and the East Asian summer monsoon precipitation. *AcMeS* 27(5):716–724
- Wu G, Duan A (2013) Extreme weather and climate changes and its environmental effects over the Tibetan Plateau. *Chinese Journal of Nature* 35(3):167–171
- Wu Q, Zhang T (2008) Recent permafrost warming on the Qinghai-Tibetan Plateau. *J Geophys Res* 113(D13). <https://doi.org/10.1029/2007JD009539>
- Yang M, Nelson FE, Shiklomanov NI, Guo D, Wan G (2010a) Permafrost degradation and its environmental effects on the Tibetan Plateau: a review of recent research. *Earth Sci Rev* 103(1–2):31–44. <https://doi.org/10.1016/j.earscirev.2010.07.002>
- Yang M, Yao T, Gou X, Hirose N, Fujii HY, Hao L, Levia DF (2007) Diurnal freeze/thaw cycles of the ground surface on the Tibetan Plateau. *Chin Sci Bull* 52(1):136–139. <https://doi.org/10.1007/s11434-007-0004-8>
- Yang Z, YH O, Xu X, Zhao L, Song M, Zhou C (2010b) Effects of permafrost degradation on ecosystems. *Acta Ecol Sin* 30(1):33–39. <https://doi.org/10.1016/j.chnaes.2009.12.006>
- Yao T (2004) Recent glacial retreat in High Asia in China and its impact on water resource in Northwest China. *Science in China Series D* 47(12):1065. <https://doi.org/10.1360/03yd0256>
- Yeşilirmak E (2014) Soil temperature trends in Büyük Menderes Basin, Turkey. *MeApp* 21(4):859–866
- Yue S, Pilon P, Cavadias G (2002) Power of the Mann-Kendall and Spearman's rho tests for detecting monotonic trends in hydrological series. *JHyd* 259(1–4):254–271
- Zhang R (2010) Trend and evolution of precipitation in Hong Kong. *Journal of HohaiUniversity(Natural Sciences)* 38(5):505–510
- Zhang T, Barry RG, Gilichinsky D, Bykhovets SS, Sorokovikov VA, Ye J (2001) An amplified signal of climatic change in soil temperature during the last century at Irkutsk, Russia. *Clim Chang* 49(1/2):41–76. <https://doi.org/10.1023/A:1010790203146>
- Zhao L, Ping C-L, Yang D, Cheng G, Ding Y, Liu S (2004) Changes of climate and seasonally frozen ground over the past 30 years in Qinghai-Xizang (Tibetan) Plateau, China. *Glob Planet Chang* 43(1–2):19–31. <https://doi.org/10.1016/j.gloplacha.2004.02.003>